Laser vaporization generation of Y $^{10}B^+$, Y $^{11}B^+$, and YAl$^+$ for electron spin resonance studies in neon matrices at 4 K: Comparison with theoretical calculations

Lon B. Knight, Jr., Robert M. Babb, Gina M. King, and Allan J. McKinley
Chemistry Department, Furman University, Greenville, South Carolina 29613

Michael D. Morse and Caleb A. Arrington
Chemistry Department, University of Utah, Salt Lake City, Utah 84112

(Received 12 November 1992; accepted 11 December 1992)

The first spectroscopic investigation of $^{89}Y\ ^{10}B^+$, $^{89}Y\ ^{11}B^+$, and $^{89}Y\ ^{27}Al^+$ is reported, revealing that both of these diatomic cation radicals have $X\ ^4\Sigma^-$ electronic ground states. The ions were generated by three high energy techniques in combination with neon matrix isolation at 4 K and studied by electron spin resonance (ESR) spectroscopy. The generation methods included pulsed laser vaporization of the metal alloys, photoionization at 16.8 eV during matrix deposition, and x-irradiation at 80 keV of the matrix sample following deposition. Hyperfine interactions were resolved for all of the above nuclei and were compared with calculated isotropic and dipolar components of the A tensor. The yttrium 5s character observed in YAl$^+$ was significantly larger than that in YB$^+$ based upon the observed nuclear hyperfine interactions. The calculated electronic structure properties showed agreement with this trend in the observed A_{iso} parameters. In addition, qualitative descriptions of the bonding properties are also presented which are consistent with the magnetic parameters obtained from the ESR measurements. The magnetic parameters for Y $^{11}B^+$ in neon at 4 K are $g_\perp = 1.959(1)$, $A_\perp$ (Y) = 33.6(4) MHz, and $A_\perp$ (^{11}B) = 65.9(4) MHz. For YAl$^+$, $g_\perp = 1.942(1)$, $A_\perp = 142(1)$ MHz, and $A_\perp$ (Al) = 73(1) MHz.

INTRODUCTION

The diatomic radicals Y $^{11}B^+$, Y $^{10}B^+$, and YAl$^+$ have been generated by pulsed laser vaporization of their corresponding alloys and trapped in neon matrices as isolated ions at 4 K for electron spin resonance (ESR) investigation. The x-irradiation (80 keV) of the deposited matrix samples was observed to significantly increase the yield of these cation radicals; photoionization at 17 eV during the deposition process produced only small increases. While no previous spectroscopic or theoretical studies have been reported for YB$^+$ or YAl$^+$, these ESR results clearly establish their electronic ground states as $^4\Sigma^-$. The five valence electrons are assigned to the molecular orbital arrangement of ... $1\sigma^2\ 2\sigma^1 1\pi^2$ with the three unpaired electrons in bonding orbitals. The nuclear hyperfine interactions (A tensors) observed for $^{89}Y(I = \frac{1}{2})$, $^{10}B(I = 3)$, $^{11}B(I = \frac{3}{2})$, and $^{27}Al(I = \frac{5}{2})$ provide direct information concerning the distribution of the spin density in the various atomic orbitals. A nonrelativistic CI type *ab initio* calculation of the nuclear A tensors was conducted as part of this experimental study. While the absolute agreement with experiment was poor, the calculations did reflect the observed trend in these hyperfine parameters. Large basis set calculations at the highest levels of theory have demonstrated agreement within approx. 10–15 % of the observed values for the isotropic and dipolar nuclear hyperfine interactions for small radicals composed of atoms in the first and second rows.[1–5] However, very few, if any, high level attempts have been made to calculate such properties for radicals containing atoms as complex as yttrium. Given the importance of understanding superconductivity and other phenomena in heavy atom materials, the development of such computational and theoretical approaches is obviously receiving considerable attention. The calculation of spin densities and electronic ground states represent difficult challenges even for small heavy metal radicals given the density of states involved. Information learned in the process will be useful in the development of models for larger molecules and perhaps even for important solid state materials.

The possible thin film applications of Y_xB_y and Y_xAl_y make information concerning the vapor phase composition above these alloys especially significant.[6] Of specific interest is the existence of YB_6 as a superconductor[6–9] in thin films produced by sputtering.[10] The YB_6 material produced by plasma deposition also has potential as a high temperature solar energy absorbing surface.[11] The manufacture of high thermal conductivity AlN involves the atomization of an Al/Y mixture in the presence of nitrogen. In the final AlN composite, the yttrium content seems to significantly increase the thermal conductivity over the nondoped compound.[12] Effusion oven mass spectrometric studies have yielded dissociation energies for a few intermetallic yttrium compounds.[13] As well as NMR studies, there have also been theoretical calculations conducted on the thermodynamic properties of YAl solids with much less attention given to YB.[14–16] Several calculations have been conducted on the bonding of transition metals to nontransition metals including boron and aluminum in bulk solids.[17]

The rare gas ESR matrix isolation approach has been reviewed for neutral and ion radicals in previous reports.[18–21] The yttrium radicals investigated by this method

 0021-9606/93/064404-09$06.00 © 1993 American Institute of Physics

Downloaded 02 Apr 2001 to 128.110.196.147. Redistribution subject to AIP copyright, see http://ojps.aip.org/jcpo/jcpcr.jsp

are $Y\,^{16}O$ (Ref. 22), $Y\,^{17}O$ (Ref. 23), YS (Ref. 24), YH_2 (Ref. 25), Y_3 (Ref. 26), YF_2, $Y(CN)_2$ (Ref. 27), HYOH (Ref. 23), YNi, and YPd.[28] In some cases, it has been found that the direct trapping of the plasma produced in the laser vaporization of materials can yield a sufficient number of isolated cation and anion radicals in the rare gas matrix for ESR detection.[21] Examples of radicals where this has been demonstrated include Si_2^+,[29] $GaAs^+$, and GaP^+.[30] As described in the experimental section, such direct ion trapping was also observed in these laser vaporization studies of YB^+ and YAl^+.

EXPERIMENT

Four different high energy generation and trapping procedures for ESR studies of isolated ion radicals in neon hosts have been used in our laboratory in recent years. The specific term "isolated ion" is used to describe the trapping of cations and anions in different lattice sites separated by an indeterminant number of rare gas atoms.[31] It has been shown that molecular cation radicals trapped in highly dilute neon matrices under such conditions yield g and A tensor results which are shifted only 1–3 % from gas phase measurements. However, the only cases where gas-matrix comparisons can be made are N_2^+, H_2O^+, and $^{13}CO^+$.[21] Neon matrix ion generation methods include electron bombardment (50–70 eV), photoionization (17 eV), pulsed laser vaporization and x-irradiation in the 20–100 keV range.[20,21,32–34] In some studies, a combination of these techniques has been employed to produce the desired ion radical. For example, C_2^+ was produced by the pulsed laser vaporization of graphite in combination with photoionization at 17 eV for a detailed study of the ESR spectra of $^{12,13}C_2^+$ ($X\,^4\Sigma$).[35]

The experimental arrangement used in this YB^+ and YAl^+ investigation is similar to that employed in our previous study of Si_2^+ and Ge_2^+.[29] A simplified diagram of the matrix apparatus, which can simultaneously accommodate laser vaporization, photoionization, and x-irradiation, is shown in Fig. 1. One advantage of using more than one ion generation method in the study of a given radical is the independent confirmation of the spectral assignment. Moreover, there is usually a wide variation in the number of desired ions produced by the different methods and the ability to predict which technique will be most appropriate for a given molecule is practically impossible.

The $YB_{(s)}$ and $YAl_{(s)}$ alloys were formed from a mixture of the elements in an electric arc furnace operating in an argon atmosphere. The same procedure was used to produce the sample of $Y\,^{10}B$ which was enriched to 94% in ^{10}B over its natural abundance of 20%. The high purity metals and enriched boron were purchased from Alfa. These alloy targets were mounted 5 cm from the copper rod matrix deposition surface, which was maintained at 4 K by a closed cycle helium refrigerator (APD-304 HS). The frequency doubled output from a Nd:YAG laser operating at 10 Hz and 25 mJ per pulse was focused to a spot size of approximately 0.4 mm. Using an external lens, the vaporization beam was moved across the target during a typical 30 min deposition with the neon flow maintained at 5 std. $cm^3\ min^{-1}$. Following deposition, the matrix sample was lowered into the X-band ESR cavity by a hydraulic system which supports the helium cryostat.

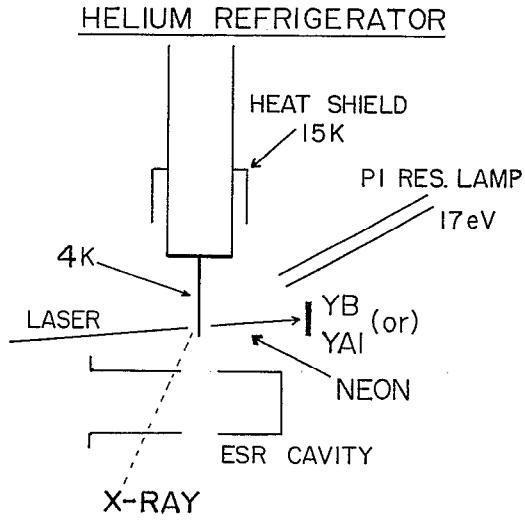

FIG. 1. The ESR matrix isolation apparatus used in these YB^+ and YAl^+ studies is shown. The relative positions of the laser vaporization targets (YB or YAl), the x-irradiation source and the open tube neon resonance photoionization lamp (16.8 eV) are schematically indicated. Following deposition, a hydraulic system allowed the matrix sample to be lowered into the X-band microwave cavity, which employed 100 kHz modulation. The electromagnet (9 in. pole face with a 4 in. gap) is mounted on tracks and can be rolled into position after deposition and/or x irradiation is completed. The magnet is not shown in this diagram.

In other ion trapping experiments and in cases of small neutral radicals, we have found that precooling the neon matrix gas to approximately 15–20 K improves the trapping efficiency. The experimental details of such precooling, achieved by passing the neon gas through a coil attached to the radiation shield of the cryostat, have been described previously.[36]

A small increase (approx. 15–20 %) in the cation radical ESR signals assigned to YB^+ and YAl^+ was observed if the matrix was irradiated at 16.8 eV using a neon resonance photoionization lamp during the deposition process (see Fig. 1). A considerably larger increase (200%) in ESR signals was observed if the matrix sample was x-irradiated after deposition for 30 min at 80 keV. The equipment and procedure used in our laboratory for x-ray generation of radical ions in rare gas hosts have been described in a recent report on the CH_3OH^+ cation radical.[33] A major advantage of the x-ray method is that it can be applied after matrix deposition and isolation of the neutral precursor has been completed. In contrast, photoionization at 16.8 eV must be conducted during the deposition process, and this seems to generate a greater level of background impurity radicals compared to the x-irradiation method of ion generation.

The identity of the counter anion in these studies could not be determined. However, background H_2O^+ and H atom ESR signals were quite intense, suggesting that significant amounts of OH^- could be present. In previous

Downloaded 02 Apr 2001 to 128.110.196.147. Redistribution subject to AIP copyright, see http://ojps.aip.org/jcpo/jcpcr.jsp

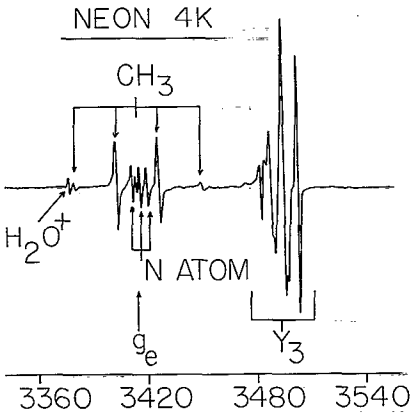

FIG. 2. ESR absorptions in the g_e magnetic field region are shown for one of the YAl^+ deposition experiments. This spectrum was recorded after vaporization products from a YAl sample were isolated in a neon matrix at 4 K. The signal amplification level of this spectrum is approximately 100 times less than that employed to detect YAl^+ in the 1740 G magnetic field region. See Fig. 4. The yttrium trimer (Y_3) and background radicals commonly detected in such high energy trapping experiments are denoted.

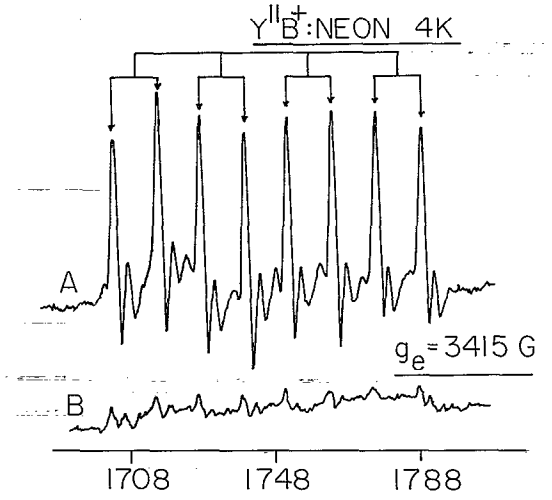

FIG. 3. The ESR spectrum assigned to the $M_S=\frac{1}{2}\leftarrow M_S=-\frac{1}{2}$ transition of $^{89}Y\ ^{11}B^+$ in its ground $^4\Sigma$ state is shown. The perpendicular ($\Theta=90°$) absorption exhibits nuclear hyperfine structure consisting of a $^{11}B(I=\frac{3}{2})$ quartet of $^{89}Y(I=\frac{1}{2})$ doublets. The $Y\ ^{10}B^+$ spectrum shown in Fig. 4 confirms this hyperfine assignment. The lower trace labeled *B* was recorded under the same conditions as *A* but after 45 min of visible light photolysis. The signal decrease indicates that an isolated ion radical is responsible for the ESR absorptions.

experiments, the presence of isolated anion radicals has been established by doping the matrix with appropriate neutral molecules. Specific examples of radical anions detected in neon matrices include F_2^- (Ref. 37), CH_2^- (Ref. 38), and CO_2^-.[23]

RESULTS

The experimental observations can be summarized in the following manner. The ESR signals assigned to YB^+ and YAl^+ were observed by trapping the products produced by the laser vaporization of $YB_{(s)}$ and $YAl_{(s)}$ in neon matrices at 4 K. The intensity of these absorptions was significantly enhanced by x-irradiation of the matrix after deposition; photoionization during deposition produced only slight signal increases. All attempts to observe these radical cations in argon matrices were unsuccessful. This failure suggests that the ion formation mechanism might involve the codeposition reaction of Y^+ with B(or Al), a process that would be more hindered with argon relative to neon due to reduced diffusion rates in argon. The x-ray ionization of neutral YB or YAl also present in the matrix presumably accounts for the increase in the cation radical signals upon x-irradiation. Direct evidence that diffusion type reactions were occurring under these neon matrix deposition conditions was the observation of intense Y_3 ESR signals which have been previously analyzed and assigned.[26] These earlier experiments utilized conventional high temperature effusion ovens for the generation of Y_3 by the matrix deposition of a high flux of Y atoms. It is interesting that pulsed laser vaporization also produced this small cluster species. An ESR spectrum recorded in the g_e magnetic field region is shown in Fig. 2 where the Y_3 signals dominate (Y_3 has a $^2B_2$ electronic ground state).

For a ground $^4\Sigma$ electronic state with a large D value (zfs) relative to the microwave quantum ($h\nu$) employed in the X-band ESR measurements, the perpendicular ($\Theta=90°$) fine structure transition corresponding to $M_S=\frac{1}{2}\leftarrow M_S=-\frac{1}{2}$ should be observed in the $g=4$ magnetic field region. Simulated line shapes and a detailed analysis of such a transition for a powder sample have been described in the recent GaP^+ report[30] and elsewhere.[18] Moderately intense absorption features were observed in this field region for the YB and YAl depositions as shown in Figs. 3 and 4, respectively.

The $^{89}Y\ ^{11}B^+$ experiments yielded an equally spaced eight line nuclear hyperfine pattern which could either be a $^{89}Y(I=\frac{1}{2})$ doublet of $^{11}B(\frac{3}{2})$ quartets or a quartet-of-doublets pattern. Experiments with isotopically enriched $^{10}B(I=3)$ were required to remove this ambiguity. The ESR results for $^{89}Y\ ^{10}B^+$ are shown in Fig. 5 where a clear yttrium doublet of 12 G (Gauss) is further split into ^{10}B septets with an A value of 8 G. These results show why the $^{89}Y\ ^{11}B$ case fortuitously exhibited eight equally spaced lines. The ^{10}B splitting of 8 G may be converted to a splitting of 24 G for ^{11}B using their g_N ratios. A yttrium doublet of 12 G and a ^{11}B quartet of 24 G will produce the equally spaced eight line pattern initially observed for $Y\ ^{11}B^+$.

For the $^{89}Y\ ^{27}Al^+$ ESR spectrum, an unambiguous Y doublet of $^{27}Al(I=\frac{5}{2})$ sextets was observed (see Fig. 4). Using our previously described diagonalization programs,[30,35] exact solutions to the following spin Hamiltonian were used to extract the magnetic parameters:

$$\hat{H}=\beta_e\bar{H}\cdot\hat{g}\cdot\bar{S}+D[S_z^2-S(S+1)/3]+\bar{I}\cdot\hat{A}\cdot\bar{S},$$

Downloaded 02 Apr 2001 to 128.110.196.147. Redistribution subject to AIP copyright, see http://ojps.aip.org/jcpo/jcpcr.jsp

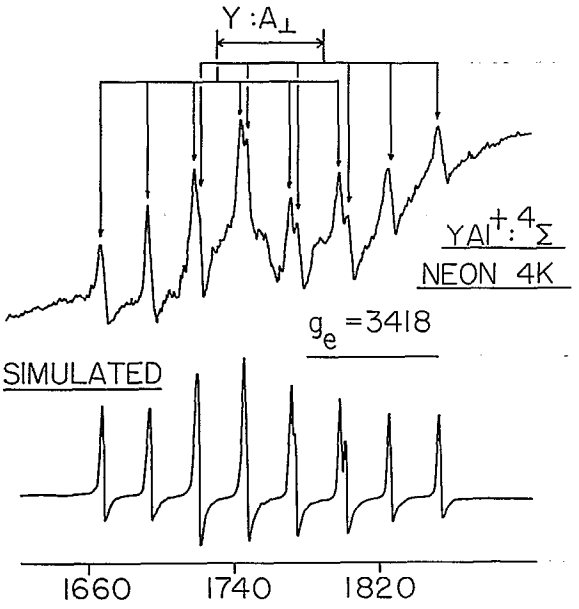

FIG. 4. The upper ESR spectrum is assigned as the perpendicular absorptions for the $M_S=\frac{1}{2}\leftarrow M_S=-\frac{1}{2}$ transition of YAl^+ in its ground $^4\Sigma$ state. The $^{89}Y(I=\frac{1}{2})$ doublet of $^{27}Al(I=\frac{5}{2})$ sextets reflects the nuclear hyperfine interaction. The lower trace is a simulated ESR spectrum using the magnetic parameters listed in Table II.

where all symbols have their standard meanings and the hyperfine terms involving both magnetic nuclei are included.[18] The observed line positions assigned to $Y\ ^{10}B^+$, $Y\ ^{11}B^+$, and YAl^+ are listed in Table I. Calculated lines agreed with the observed positions within the experimental uncertainty of ± 0.5 G. It was not necessary to include boron or aluminum quadrupole terms in the spin Hamiltonian to obtain the agreement. The magnetic parameters obtained by this line fitting procedure are listed in Table II. A simulated spectrum of YAl^+, showing excellent agreement with the observed spectrum, is shown in the lower trace of Fig. 4.

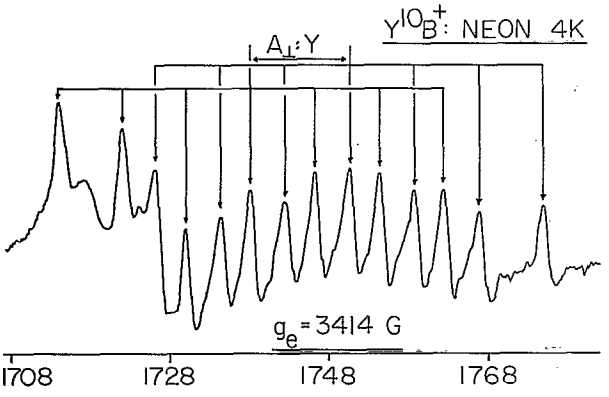

FIG. 5. The ESR spectrum of $^{89}Y\ ^{10}B^+$ trapped in a neon matrix at 4 K is shown. The nuclear hyperfine pattern reveals a $^{89}Y(I=\frac{1}{2})$ doublet of $^{10}B(I=3)$ septets for this $^4\Sigma^-$ ground state ion radical. This spectrum should be compared with the $^{11}B(I=\frac{3}{2})$ quartet of Y doublets shown in Fig. 2.

Since only one fine structure line is observed, it is not possible to obtain the $g_\perp$ and D values independently from the experimental results alone. Holding the observed line positions constant, the relationship between D and $g_\perp$ is graphically presented for YAl^+ in Fig. 6. The relationship between D and $g_\perp$ for YB^+ is similar. It is a reasonable assumption that for such a heavy atom radical, the D value far exceeds 5 cm^{-1} because of the potentially large spin–orbit contribution to D.[18] For such a case, the $g_\perp$ value can be accurately determined as shown by this plot. For $D>5$ cm^{-1}, the $g_\perp$ value for YB^+ is 1.959(1) and 1.942(1) for YAl^+. A greater $g_\perp$ shift from g_e would be expected for YAl^+ than for YB^+, since spin–orbit interaction between $X\ ^4\Sigma^-$ and excited regular $^4\Pi_r$ and $^2\Pi_r$ states would be larger in the case of aluminum due to its larger atomic spin–orbit parameter (75 cm^{-1} for Al, as compared to 11 cm^{-1} for B). The involvement of valence p_z character on boron and aluminum is qualitatively indicated by this observed $g_\perp$ trend. A more quantitative g tensor analysis is not possible without excited state energies and wave functions. The g shift in the YO ($X\ ^2\Sigma$) radical is much smaller with $g_\perp=2.001$, despite the relatively large spin–orbit parameter of yttrium.[22,23] The smaller $g_\perp$ values for YB^+ and YAl^+ also suggests that the $^2\Pi_r$ and $^4\Pi_r$ states responsible for this shift lie lower in YB^+ and YAl^+ than in YO.

DISCUSSION

The assignment of the observed ESR spectra to ground $^4\Sigma^-$ states of YB^+ and YAl^+ is based upon definitive nuclear hyperfine patterns, the characteristic magnetic field location of the absorption for a $^4\Sigma^-$ state with D large relative to $h\nu$, the use of three independent ion generation methods, and the sample response to photolysis with visible light (photobleaching). The effect of photobleaching on the YB^+ ESR spectrum is shown in the lower trace of Fig. 3, where irradiation with visible light for 40 min practically eliminated the ESR signals. This is the expected behavior for isolated cations and anions in the rare gas host, since photoionization of the anion releases an electron which can readily diffuse throughout the neon lattice and neutralize the cation radical. It is unlikely that visible light would photochemically dissociate a neutral YB molecule trapped in the rare gas lattice. Moreover, the electronic ground state of neutral YB (or YAl) would likely be $^3\Sigma^-$, $^3\Pi$, or a singlet state. ESR would not detect a singlet state and $^3\Sigma^-$ absorptions would not exhibit absorption lines in the $g=4$ region at X-band microwave frequencies because of the large D value expected for these molecules. A $^3\Pi$ state would also not likely be detected in rare gas matrices because of the line broadening that would result from the extreme g and D tensor anisotropy. In addition to these considerations, resonant two-photon ionization spectroscopy of YAl has detected a band system near 9500 cm^{-1}, and a preliminary analysis of the rotational structure suggests that the ground state is a $^3\Sigma^-$ state with a large zero-field splitting (D).[39] On these grounds we are confident in our assignment of the observed spectra to the cation radicals YB^+ and YAl^+, rather than to the neutral parent molecules.

Downloaded 02 Apr 2001 to 128.110.196.147. Redistribution subject to AIP copyright, see http://ojps.aip.org/jcpo/jcpcr.jsp

TABLE I. ESR line positions (Gauss) for $^{89}Y\ ^{10}B^+$, $^{89}Y\ ^{11}B^+$, and $^{89}Y\ ^{27}Al^+$ in neon matrices at 4 K. Calculated line positions agree with these observed values within the experimental uncertainty of ±0.5 G using the magnetic parameters in Table II and an exact diagonalization solution to the spin Hamiltonian.

Y (M_I)	^{10}B (M_I)	$^{89}Y\ ^{10}B^+$ Observed[a]	^{11}B (M_I)	$^{89}Y\ ^{11}B^+$ Observed[b]	^{27}Al (M_I)	$^{89}Y\ ^{27}Al^+$ Observed[c]
1/2	3	1714	$\frac{3}{2}$	1704	$\frac{5}{2}$	1667
	2	1722	$\frac{1}{2}$	1728	$\frac{3}{2}$	1692
	1	1730	$-\frac{1}{2}$	1752	$\frac{1}{2}$	1720
	0	1738	$-\frac{3}{2}$	1776	$-\frac{1}{2}$	1747
	−1	1746			$-\frac{3}{2}$	1774
	−2	1754			$-\frac{5}{2}$	1802
	−3	1762				
−1/2	3	1726	$\frac{3}{2}$	1716	$\frac{5}{2}$	1718
	2	1734	$\frac{1}{2}$	1740	$\frac{3}{2}$	1744
	1	1742	$-\frac{1}{2}$	1764	$\frac{1}{2}$	1771
	0	1750	$-\frac{3}{2}$	1789	$-\frac{1}{2}$	1798
	−1	1759			$-\frac{3}{2}$	1825
	−2	1767			$-\frac{5}{2}$	1853
	−3	1775				

[a]Microwave freq.=9568.3(3) MHz.
[b]Microwave freq.=9570.9(3) MHz.
[c]Microwave freq.=9570.3(3) MHz.

A preliminary understanding of the electronic structure of YB^+ and YAl^+ may be obtained by considering the orbital energies of the component atoms (or atomic ions). An examination of tables of atomic energies shows that it requires 50 144 cm^{-1} of energy to remove the $4d$ electron from the $4d^15s^2$, ^2D ground state of Y,[40] while an energy of approximately 52 315 cm^{-1} is required to remove a $5s$ electron (averaging the energies of the ^1D and ^3D states of the resulting Y^+ ion).[41] Thus, the $4d$ and $5s$ orbitals are essentially degenerate in atomic yttrium, and both must certainly be considered in describing the bonding of such molecules as YB^+ and YAl^+. In contrast, 66 912 cm^{-1} of energy is required to remove the $2p$ electron of boron, while approximately 122 280 cm^{-1} is required to remove the $2s$ electron (again averaging the energies of the ^1P and ^3P states of the resulting B^+ ion).[41] Because the $2s$ electrons are so strongly bound in the boron atom, we may consider them as part of the core, and they may be omitted from consideration in forming the molecular orbitals of the YB^+ molecule. Similar considerations show that the $3p$ electron of aluminum is bound by 48 278.5 cm^{-1}, while the $3s$ electrons are bound by approximately 96 930 cm^{-1} (again averaging the energies of the ^1P and ^3P states of the resulting Al^+ ion).[41] As in the boron atom, the high binding energy of the $3s$ electrons of aluminum is expected to cause them to remain corelike, and to contribute minimally toward the bonding in the molecule. Accordingly, they may be omitted from initial consideration in forming the molecular orbitals of the YAl^+ molecule.

With the exclusion of the filled B($2s$) and Al($3s$) atomic orbitals from consideration as valence orbitals, the bonding in YB^+ (YAl^+) will result from the placement of three electrons in molecular orbitals primarily derived from the Y($5s$), Y($4d$), and B($2p$) [or Al($3p$)]

TABLE II. Observed magnetic parameters (MHz) for YB^+ and YAl^+ in their $X\,^4\Sigma$ states isolated in neon matrices at 4 K.

	$^{89}Y\ ^{10}B^+$	$^{89}Y\ ^{11}B^+$	$^{89}Y\ ^{27}Al^+$
$g_\perp$ [a]	1.969–1.960	1.968–1.959	1.951–1.942
$A_\perp$ (^{89}Y)[b]	33.6(4)	33.6(4)	142(1)
$A_\perp$ (B or Al)[b]	22.1(2)	65.9(4)	73(1)

[a]The indicated $g_\perp$ range reflects a D(zfs) value between 1 and 5 cm^{-1} for the observed line positions of Table I. For D greater than approximately 5 cm^{-1}, which is most probably the case for these radicals, $g_\perp$ remains essentially at the lower limit listed in this table. See text and Fig. 5.
[b]Given the small calculated magnitudes of A_{dip}, these measured $A_\perp$ values are approximately equal to A_{iso}.

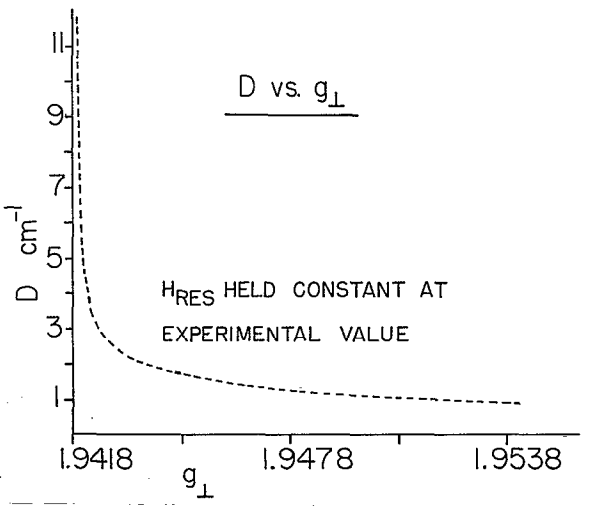

FIG. 6. The relationship between the D parameter (zfs) and the $g_\perp$ value for a $^4\Sigma$ radical is plotted under the condition of holding the observed line positions constant. The specific data analyzed in this example is for the YAl^+ cation radical in its $^4\Sigma^-$ ground state (see the experimental line positions in Table I). Note that for D greater than approximately 5 cm^{-1}, the $g_\perp$ parameter is well determined. In this case the limiting $g_\perp$ is 1.942 (see Table II).

Downloaded 02 Apr 2001 to 128.110.196.147. Redistribution subject to AIP copyright, see http://ojps.aip.org/jcpo/jcpcr.jsp

atomic orbitals. With the Y(5*s*) and Y(4*d*) orbitals nearly degenerate in the isolated yttrium atom, this set of atomic orbitals will lead to three σ orbitals (which may be described as bonding, nonbonding, and antibonding, respectively), two pairs of π orbitals (one bonding and one antibonding), and a single pair of nonbonding δ orbitals. In either YB^+ or YAl^+ it is expected that the bonding orbitals should lie below the nonbonding or antibonding orbitals, giving $1\sigma^2 2\sigma^1 1\pi^2$ as the orbital configuration of the observed $^4\Sigma$ ground state. In this notation the 1σ orbital represents the B(2*s*) or Al(3*s*) core orbital, which we have assumed to be uninvolved in the chemical bonding. The 2σ orbital is expected to be a bonding orbital, primarily composed of the $5s\sigma_Y$, $4d\sigma_Y$, and $2p\sigma_B$ (or $3p\sigma_{Al}$) orbitals, while the 1π orbital is a bonding combination of the $4d\pi_Y$ and $2p\pi_B$ (or $3p\pi_{Al}$) orbitals. Owing to the greater electronegativity of boron as compared to aluminum, one would expect less yttrium character in the 2σ and 1π orbitals of YB^+ than in YAl^+

This picture of the basic electronic structure of YB^+ and YAl^+ is supported by the measured nuclear hyperfine splittings and by electronic structure calculations reported in the next section. Of course, for a $^4\Sigma^-$ state to be the ground state, the 2σ and 1π orbital energy levels must be close in energy. This, combined with the fact that the 2σ and 1π orbitals are bonding orbitals in these molecules, makes the YB^+ and YAl^+ molecules somewhat similar to the previously studied GaP^+ (Ref. 30), Si_2^+ (Ref. 29) BC (Ref. 5), and C_2^+ (Ref. 35) molecules, where detailed analyses of the A tensors for a $^4\Sigma^-$ state deriving from a $\sigma^1\pi^2$ configuration have been presented. A similar treatment for YB^+ and YAl^+ cannot be as complete since only the $A_\perp$ hyperfine parameters could be directly measured in these samples. However, $A_\perp$ is a reasonable approximation for A_{iso} since $A_{iso}=A_\perp+A_{dip}$, and the theoretical calculations show A_{dip} to be very small (only a few MHz). A qualitative explanation of why A_{dip} is expected to be small in these radicals is presented below. For the present we will simply use the relation $A_{iso}\approx A_\perp$ to estimate the valence "*s*" orbital character.

The singly occupied 2σ orbital for YB^+ and YAl^+ can be expressed in terms of the simple linear combination atomic orbitals (LCAO):

$$\psi_\sigma = C_{5s}X_{5s}+C_{4dz^2}X_{4dz^2}+C_{ns}X_{ns}+C_{npz}X_{npz}+\cdots,$$

where $n=2$ for boron and 3 for aluminum. Of course, yttrium $5p_z$ and other σ type basis functions are also involved to various extents. The amount of 5*s* yttrium character can be estimated from the commonly applied free atom comparison method (FACM) using the tabulated atomic yttrium A_{iso} value of 1250 MHz.[42] The atomic A_{dip} parameter for the $4d_{z^2}$ orbital of yttrium is only 18 MHz.[42] For small radicals containing atoms in the first three rows, the FACM approach has been found to yield generally consistent results in reasonable agreement with high level calculations in estimating the orbital characters of the unpaired electrons. A detailed analysis of the various approximations involved and a comparison with *ab initio* theoretical results have been presented in a previous report on the $^{29}SiO^+$ cation radical.[4] The FACM approach has not been rigorously analyzed for the heavier elements with a larger number of inner shells and the need for including relativistic effects.

The A values actually measured and calculated in the MELDF program described later reflect a total spin density normalized to unity, even though there are three unpaired electrons. The FACM estimate of the yttrium 5*s* character in the 2σ orbital of YB^+ is 34 MHz/1250 MHz=0.03; in YAl^+ it is 142/1250=0.11. Similarly, the boron 2*s* character is 0.03 and the aluminum 3*s* character is 0.02, using ^{11}B and ^{27}Al atomic A_{iso} values of 2550 and 3910 MHz, respectively.[42] The approximation $A_{iso}=A_\perp$ has been used. These A_{iso} FACM estimates, especially for yttrium, should be considered highly approximate in nature. For example, the use of Koh and Miller's atomic A_{iso} parameter for yttrium of 650 MHz causes the above FACM estimates for the Y(5*s*) characters to be increased by approximately a factor of 2.[42] Use of the smaller atomic A_{iso} value for the yttrium atom yields considerably better agreement with the calculated spin populations presented in the theoretical section of this report. It should also be noted that no attempt is being made to use charge corrected atomic A_{iso} parameters in this FACM approach.

For YAl^+, it is possible to estimate the $A_\parallel$ hyperfine parameter for aluminum from its higher order effects on the observed perpendicular hyperfine spacings. The extremely weak parallel type absorptions occur in the g_e region, which is obscured by intense background radical signals. Considerable effort was expended to measure carefully and analyze the perpendicular spacings between the Al:$M_I=\frac{5}{2}$ and $\frac{3}{2}$ lines of the Y:$M_I=\frac{1}{2}$ transition and the Al:$M_I=-\frac{5}{2}$ and $-\frac{3}{2}$ lines of the Y:$M_I=-\frac{1}{2}$ transition. As seen by the YAl^+ ESR spectrum in Fig. 4, these four lines are the only ones which are not overlapped by other transitions and they are also the best candidates for determining the $A_\parallel$ value from the perpendicular line positions. The difference between these differences reflects the higher order "spread" or increase in the Al sextet hyperfine spacing as M_I varies from $+\frac{5}{2}$ to $-\frac{5}{2}$. For $A_\parallel=A_\perp=73$ MHz for Al, this "difference" is 1.0 G as calculated using the exact diagonalization treatment. Independent, high resolution measurements on six different matrix depositions indicate a difference of at least 1.2 G. Quadrupole interactions and D value changes were examined to show that this small "difference" depended only upon the $A_\parallel$ parameter once $A_\perp$ was established. Computed line positions show that a "difference" of 1.2 G requires that $A_\parallel=100$ MHz. Using this result, an Al A_{dip} value of 9 MHz is obtained from the expression, $A_{dip}=(A_\parallel-A_\perp)/3$. If the dipolar interaction on aluminum is dominated by spin density in its $3p_z$ orbital, the FACM estimate of this orbital character would be 0.33 using an A_{dip} atomic value for aluminum of 83 MHz.[42] However, the aluminum dipolar interaction would also be influenced by spin density residing in the Al $3p_x$ and $3p_y$ orbitals. Spin density on yttrium would make only a small contribution given the r^{-3} dependence. For YB^+, the $^{10,11}B$ hyperfine splitting was too small to obtain the $A_\parallel$ parameter from the perpendicular lines.

Downloaded 02 Apr 2001 to 128.110.196.147. Redistribution subject to AIP copyright, see http://ojps.aip.org/jcpo/jcpcr.jsp

Most of the spin density in the π_x and π_y molecular orbitals should reside in the d_{xz} and d_{yz} yttrium orbitals and the boron and aluminum np_x and np_y orbitals. An estimate of the relative distributions of the spin density among these orbitals for YB^+ and YAl^+ will be presented in the following theoretical section.

THEORETICAL CALCULATIONS

GAUSSIAN 90 calculations, using the STO 3G* basis set at the UHF level, yielded optimized bond distances of 2.262 and 2.686 Å for YB^+ and YAl^+, respectively.[43] This compares to a ground state bond length measured for the $X\,^3\Sigma_0^-$ state of neutral YAl of 2.812(3) Å (uncorrected for spin-uncoupling effects).[39] Calculated GAUSSIAN 90 bond distances at the restricted open-shell Hartree Fock (ROHF) level were found to be 2.204 and 2.667 Å for YB^+ and YAl^+ respectively. Bond distances, calculated with a modified version of the MELDF suite of programs at the ROHF level, yielded similar results.[44] All of the calculations are highly approximate and preliminary in nature given the low level and small basis set employed and the neglect of relativistic effects.

On the quartet manifold, the $^4\Sigma^-$ state was found to be the lowest in energy for both ions, while $^2\Pi$ states ($1\sigma^2 2\sigma^2 1\pi^1$ and $1\sigma^2 1\pi^3$) were lowest on the doublet manifold. Both the MELDF and GAUSSIAN 90 calculations predict the electronic ground state to be $X\,^4\Sigma^-$ for YB^+ and YAl^+, in agreement with the experimental observations. Given the highly approximate nature of the calculations, the properties and energies of the excited states are most probably of little quantitative significance. The potential energy curves for the two types of pi states ($^2\Pi_i$ and $^2\Pi_r$) cross in the vicinity of the optimized ground state bond distance. Since the measured $g_\perp$ values for both ions are less than g_e, dominant spin–orbit coupling to excited $^2\Pi_r$ or to $^4\Pi_r$ states is indicated.[18]

The calculated energy difference between the σ and π levels in the $X\,^4\Sigma^-$ state was quite sensitive to the bond distance employed. For YB^+ the σ level was 0.0718 hartrees below the π levels for $r=2.250$ Å as determined by the MELDF program at the ROHF level. For YAl^+ at 2.700 Å, the π levels were 0.0081 hartrees below the σ level.

As previously discussed in an experimental-theoretical analysis of the $^{29}SiO^+$ radical cation, the MELDF program has the capability to project the calculated spin density onto a minimal basis set to facilitate a simple valence orbital description.[4] The gross MSPA (Milliken spin population analysis) results, reflecting the $(\alpha-\beta)$ spin differences, are presented for the various valence orbitals indicated. For YB^+, $Y_{5s}=0.08$, $Y_{4dz^2}=0.01$, $Y_{4yz}=Y_{4xz}=0.21$, $B_{2s}=0.08$, $B_{2pz}=0.16$, and $B_{2px}=B_{2py}=0.11$, where 0.97 of the total spin density, normalized to unity, is included. The obvious symmetries of these orbitals allow spin density assignments to be made to the molecular σ and $\pi_{x,y}$ types in the $X\,^4\Sigma^-$ state. For YAl^+, $Y_{5s}=0.24$, $4d_{z^2}=0.01$, $4d_{yz}=4d_{xz}=0.26$, $Al_{3s}=0.03$, $Al_{3pz}=0.07$, and $Al_{3py}=Al_{3py}=0.05$ where the sum is again 0.97. Given symmetry restrictions in these MSPA routines, the partitioning of the spin density between the Y_{5s} and Y_{4dz^2} orbitals is highly approximate, although the sum of these two contributions is properly analyzed. These MELDF MSPA results and the calculated nuclear hyperfine interactions (A tensors) discussed below were conducted at the multireference single, double, configuration interaction (MRSDCI) level involving 40 reference configurations which included all single excitations. Double excitations were selected on the basis of an energy threshold criteria (E_T) which was set at $E_T=5\times10^{-8}$ hartrees. Further reductions in E_T did not significantly alter the calculated parameters.

Interpretation of the above spin populations projected onto the valence orbitals in terms of nuclear hyperfine properties is practically impossible given the potentially large effects of the inner orbitals. Therefore, a direct calculation of A_{iso} and A_{dip}, defined in the following conventional manner, was performed using the MELDF program:

$$A_{iso}=\tfrac{8}{3}\pi g_e g_n \beta_e \beta_n \langle\delta(r)\rangle,$$

$$A_{dip}=\tfrac{1}{2} g_e g_n \beta_e \beta_n \langle(3\cos^2\Theta-1)/r^3\rangle,$$

where all symbols have their standard meanings and the averages are taken over the spin densities.[18] The calculated A_{iso} parameters for yttrium in YB^+ and YAl^+ are -106 and -326 MHz, respectively. A negative A_{iso} value corresponds to positive spin density since the nuclear magnetic moment for ^{89}Y is negative. While the absolute magnitudes of these calculated A_{iso} results are significantly larger than the A_{iso} values estimated from the $A_\perp$ experimental parameters, the calculated trend does reflect the measured $A_\perp$ values of -34 and -142 MHz for YB^+ and YAl^+, respectively. As previously discussed there are several factors that could be contributing to the poor quantitative agreement. The calculated boron A_{iso} value of 155 MHz should be compared with the observed ^{11}B $A_\perp$ value of 66 MHz; for aluminum, the calculated A_{iso} was 112 MHz compared to the observed $A_\perp$ value of 73 MHz.

There is an interesting consistency in these calculated MELDF A_{iso} values derived from the total wave functions and the calculated spin population projections onto the valence atomic orbitals. Using the FACM method and the calculated MELDF A_{iso} values (as if they were experimental measurements), we obtain for YB^+ and YAl^+ 5s characters of 0.085 and 0.26, respectively, based upon the atomic A_{iso} parameter of 1250 MHz for a yttrium 5s electron. However, as mentioned previously, there is large uncertainty in the atomic yttrium A_{iso} parameter that should be employed in the FACM analysis. Additional MELDF type calculations were conducted to test for unusual sensitivity of A_{iso} to the equilibrium bond length. For YB^+ a change in length from 2.15 to 2.25 Å produced a Y A_{iso} change of approximately $+15$ MHz and a ^{11}B A_{iso} change of -1.7 MHz.

The calculated A_{dip} value was 4.7 MHz for ^{11}B in YB^+ and 1.0 MHz for ^{89}Y. For YAl^+, A_{dip} for aluminum was calculated to be 4.0 MHz and 0.75 MHz for ^{89}Y. The calculated small magnitudes of these dipolar parameters further supports the approximation of $A_{iso}=A_\perp$. It is to be expected in $\sigma^1\,\pi_x^1\,\pi_y^1$ type radicals that the dipolar hyper-

Downloaded 02 Apr 2001 to 128.110.196.147. Redistribution subject to AIP copyright, see http://ojps.aip.org/jcpo/jcpcr.jsp

fine interaction for a given nucleus will be small.[30,35] This results from the cancellation effect of the local dipolar contributions from orbitals with their symmetry axis aligned along the three different directions.[35] Of course, equal spin populations in the np_z, np_x, and np_y orbitals on a given atom would produce an A_{dip} value of zero, provided the small contribution made by spin density on other atoms is ignored. The MSPA calculations, showing similar spin densities in these p type orbitals on boron and aluminum, are thus consistent with these small calculated A_{dip} parameters.

The large increase in the observed yttrium A_{iso} value in going from YB^+ to YAl^+ reflects the larger contribution of the Y(5s) orbital to the singly occupied 2σ orbital in the latter molecule. This is probably a consequence of the similar electronegativities of the yttrium (Pauling electronegativity of 1.2) and aluminum (Pauling electronegativity of 1.5) atoms, which leads to a more nearly equal sharing of electrons than occurs in the case of the more electronegative boron (Pauling electronegativity of 2.0). Owing to the very similar electronegativities of Al(1.5) and Ga(1.6), one would expect the yttrium A_{iso} value for YGa^+ to be very similar to that found for YAl^+. In this regard, it is likely that the boron molecule YB^+ is the unusual molecule in the YB^+, YAl^+, YGa^+, YIn^+ series, and that the trends in the series YAl^+, YGa^+, YIn^+ will be smoother and more predictable.

It may come somewhat as a surprise that the ground states of YB^+ and YAl^+ are high-spin $1\sigma^2 2\sigma^1 1\pi^2$, $^4\Sigma^-$ states, rather than the low-spin $1\sigma^2 2\sigma^2 1\pi^1$, $^2\Pi_r$ or $1\sigma^2 1\pi^3$, $^2\Pi_i$ states. However, recent *ab initio* calculations by Boldyrev and Simons show that it is common for diatomic molecules composed of electropositive atoms to favor high-spin ground states.[45] These authors note, for example, that LiB is calculated to possess a $^3\Pi$ ground state deriving from the $1\sigma^2 2\sigma^1 1\pi^1$ configuration, rather than the expected $1\sigma^2 2\sigma^2$, $^1\Sigma^+$ ground state. In addition, diatomics such as LiSi and NaSi are calculated to possess ground states which place the two 3p electrons of silicon in π orbitals (as a π^2 configuration, coupled as $^3\Sigma^-$), rather than forming a two-electron bond with the 2s (or 3s) electron of Li (or Na). This again leads to $^4\Sigma^-$ ground states described as $\sigma^1\pi^2$ configurations. The same is also true of molecules such as BSi and AlSi, where once again $^4\Sigma^-$ ground states are calculated, deriving from $\sigma^2\sigma^1\pi^2$ configurations. (We have recently determined that these molecules indeed do possess $^4\Sigma^-$ ground states,[46] as calculated by Boldyrev and Simons). In these examples of a p-block element such as B or Si bonding to an electropositive element (such as Li, Na, B, or Al), the electropositive nature of the alkali (or group-III A) element makes it unfavorable to place too many electrons in σ orbitals shared between the two centers. A similar effect seems to be occurring in the YB^+ and YAl^+ molecules. It remains to be seen if these high-spin ground states persist in other transition metal molecules such as ScB^+ and $ScAl^+$, and much higher level calculations than those reported in this paper will be required to determine if the root causes of these high-spin ground states share a common origin with those of the electropositive diatomics discussed by Boldyrev and Simons.

Finally, it is of interest to compare the electronic structure of YAl^+ and YB^+ with that of the isovalent electropositive diatomic, CaAl. This molecule has also been recently investigated by resonant two-photon ionization spectroscopy, and has been found to possess a $^2\Pi_r$ ground state, rather than the $^4\Sigma^-$ ground state exhibited by YB^+ and YAl^+.[47] Considering the Ca(4s), Al(3s), and Al(3p) electrons as the valence electrons, the CaAl molecule clearly forms a ground state which may be characterized as $1\sigma^2 2\sigma^2 1\pi^1$, $^2\Pi_r$. The essential difference between this molecule and YB^+ or YAl^+ is that the 4d orbitals are quite accessible for chemical bonding in yttrium, while the 3d orbitals of calcium lie rather high in energy, and cannot form $3d\pi_{Ca}$–$3p\pi_{Al}$ bonds which are as strong as the $4d\pi_Y$–$3p\pi_{Al}$ bonds of YAl^+. Thus, although the AlCa molecule is chemically bound, and the 1π orbital definitely has some bonding character, this bonding character is not sufficient to make up for the energetic cost required to excite one of the calcium 4s electrons to the 3d orbital.

ACKNOWLEDGMENTS

Project support from the National Science Foundation (NSF) (Grant No. CHE-9019511) and the Camille and Henry Dreyfus Foundation through their Scholar-Fellow program is gratefully acknowledged. Undergraduate student support was provided by an NSF-REU site grant and a Duke Endowment grant to Furman University. Equipment funds were made available from the Monsanto Foundation, the DuPont College Science Program, and the 3M Company. Appreciation is expressed to Dr. David Feller and Professor E. R. Davidson for use of their MELDF program and to Professor Marye Anne Fox at the University of Texas (Austin) for the loan of the x-ray equipment used in these experiments. M.D.M. and C.A.A. gratefully acknowledge research support from the NSF (Grant No. CHE-8912673) and the donors of the Petroleum Research Fund.

[1] D. Feller, J. Chem. Phys. **93**, 579 (1990).
[2] S. N. Beck, E. A. McCullough, Jr., and David Feller, Chem. Phys. Lett. **175**, 629 (1990).
[3] D. Feller and E. R. Davidson, J. Chem. Phys. **80**, 1006 (1984).
[4] Lon B. Knight, Jr., A. Ligon, R. W. Woodward, David Feller, and E. R. Davidson, J. Am. Chem. Soc. **107**, 2857 (1985).
[5] Lon B. Knight, Jr., S. T. Cobranchi, J. T. Petty, E. Earl, David Feller, and E. R. Davidson, J. Chem. Phys. **90**, 690 (1989); Lon B. Knight, Jr., Brian W. Gregory, Devon W. Hill, C. A. Arrington, Takamasa Momose, and Tadamasa Shida, J. Chem. Phys. **94**, 67 (1991).
[6] James G. Ryan, Stanley, Roberts, *Thin Solid Films* **135**, 9 (1986).
[7] O. I. Shulishova and I. A. Shsherbak, Izv. Akad. Nauk SSSR, Neorg. Mater. **3**, 1495 (1967).
[8] Z. Fish, B. T. Matthias, and E. Corenzwit, Proc. Natl. Acad. Sci. **64**, 1151 (1969).
[9] S. Kunii, T. Kasuya, K. Kadowaki, M. Date and S. B. Woods, Solid State Commun. **52**, 659 (1984).
[10] R. Schneider, Kernforschungszent. Karlsruhe [Ber] KFK **4341**, 95 (1987).
[11] J. M. Schreyer, R. A. Hays, C. R. Schmitt, and D. Farwell, Sol. Energy **25**, 179 (1980).
[12] T. Kaga, Y. Nakamura, and Y. Kuranari, JPN KOAI: Tokkyo Koho JP 63, 156,007 [88,156,007].
[13] K. A. Gingerich, H. C. Finkbeiner, Proc. Rare Earth Res. Conf. 9th **2**, 795 (1971).

Downloaded 02 Apr 2001 to 128.110.196.147. Redistribution subject to AIP copyright, see http://ojps.aip.org/jcpo/jcpcr.jsp

[14] Qingsheng Ran, Hans Leo Lukas, Guenter Effenberg, Guenter Petzow, J. Less-Common Met. **146**, 213 (1989).
[15] K. A. Gschneidner, Jr., Met. Mater. Processes **1**, 241 (1990).
[16] V. P. Kalantaryan, Metallofizika **3**, 44 (1981).
[17] C. D. Gelatt, Jr., A. R. Williams, and V. L. Moruzzi, Phys. Rev. B **27**, 2005 (1983).
[18] W. Weltner, Jr., *Magnetic Atoms and Molecules* (Dover, Mineola, N.Y., 1989).
[19] P. H. Kasai, J. Am. Chem. Soc. **113**, 1539 (1991); P. H. Kasai, J. Am. Chem. Soc. **112**, 4313 (1990).
[20] Lon B. Knight, Jr., *Chemistry and Physics of Matrix-Isolated Species*, edited by L. Andrews and M. Moskovits (North-Holland, Amsterdam, 1989), Chap. 7.
[21] Lon B. Knight, Jr., *Radical Ionic Systems*, edited by A. Lund and M. Shiotani (Kluwer, Dordrecht, The Netherlands, 1991), pp. 73–97.
[22] W. Weltner, Jr., D. McLeod, and P. H. Kasai, J. Chem. Phys. **46**, 3172 (1967).
[23] Lon B. Knight, Jr. (unpublished).
[24] N. S. McIntyre, K. C. Lin, and W. Weltner, Jr., J. Chem. Phys. **56**, 5576 (1972).
[25] L. B. Knight, Jr., M. B. Wise, T. A. Fisher, and J. Steadman, J. Chem. Phys. **74**, 6636 (1981).
[26] L. B. Knight, Jr., R. W. Woodward, R. J. Van Zee, and W. Weltner, Jr., J. Chem. Phys. **79**, 5820 (1983).
[27] Lon B. Knight, Jr. and M. B. Wise, J. Chem. Phys. **73**, 4946 (1980).
[28] R. J. Van Zee and W. Weltner, Jr., Chem. Phys. Lett. **150**, 329 (1988).
[29] Lon B. Knight, Jr., J. O. Herlong, Robert Babb, E. Earl, Devon W. Hill, and C. A. Arrington, J. Phys. Chem. **95**, 2732 (1991).
[30] Lon B. Knight, Jr. and J. T. Petty, J. Chem. Phys. **88**, 481 (1988); Lon B. Knight, Jr. and John O. Herlong, J. Chem. Phys. **91**, 69 (1989).
[31] L. Andrews, Ann. Rev. Phys. Chem. **30**, 79 (1979).
[32] A. J. McKinley and J. Michl, J. Phys. Chem. **95**, 2674 (1991).
[33] Lon B. Knight, Jr., Kelley Kerr, Martha Villanueva, Allan J. McKinley, and David Feller, J. Chem. Phys. **97**, 5363 (1992).
[34] T. Bally, *Radical Ionic Systems*, edited by A. Lund and M. Shiotani (Kluwer, Dordrecht, 1991), pp. 3–52; T. Shida, E. Haselback, and T. Bally, Acc. Chem. Res. **17**, 180 (1984); K. Toriyama, K. Nunome, and M. Isasaki, J. Chem. Phys. **77**, 5891 (1982).
[35] Lon B. Knight, Jr., S. T. Cobranchi, and E. Earl, J. Chem. Phys. **88**, 7348 (1988).
[36] Lon B. Knight, Jr., John O. Herlong, Thomas J. Kirk, and C. A. Arrington, J. Chem. Phys. **96**, 5604 (1992).
[37] L. B. Knight, Jr., Edward Earl, A. R. Ligon, and D. P. Cobranchi, J. Chem. Phys. **85**, 1228 (1986).
[38] Lon B. Knight, Jr., M. Winiski, P. Miller, C. A. Arrington, and David Feller, J. Chem. Phys. **91**, 4468 (1989).
[39] C. A. Arrington, M. Doverstål, and M. D. Morse (unpublished).
[40] W. R. S. Garton, E. M. Reeves, F. S. Tomkins, and B. Ercoli, Proc. R. Soc. London, Ser. A **333**, 17 (1973).
[41] C. E. Moore, *Atomic Energy Levels*, Natl. Bur. Stand. (U.S.) Circ. No. 467 (U.S. GPO, Washington, D.C. 1949).
[42] J. R. Morton and K. F. Preston, J. Magn. Reson. **30**, 577 (1978); A. K. Koh and D. J. Miller, At. Data Nucl. Data Tables **33**, 235 (1985).
[43] GAUSSIAN 90, Revision G, M. J. Frisch, M. Head-Gordon, G. W. Tucks, J. B. Forseman, H. B. Schlegel, K. Raghavachari, M. Robb, J. S. Binkley, C. Gonzalez, D. J. Defrees, D. J. Fox, R. A. Whitehead, R. Seeger, C. F. Melius, J. Baker, R. L. Martin, L. R. Kahn, J. J. P. Stewart, S. Topiol, and J. A. Pople, Gaussian, Inc., Pittsburgh, PA 1990.
[44] MELDF was originally written by L. McMurchie, S. Elbert, S. Langhoff, and E. R. Davidson. It has been substantially modified by D. Feller, R. Cave, D. Rawlings, R. Frey, R. Daasch, L. Nitzche, P. Phillips, K. Iberle, C. Jackels, and E. R. Davidson. Further modifications were made in our laboratory by the addition of the STO 3G* basis functions for yttrium and its g_N factor for the nuclear hyperfine calculations.
[45] A. I. Boldyrev and J. Simons, J. Phys. Chem. (to be published).
[46] L. B. Knight, Jr., R. M. Babb, A. J. McKinley, M. D. Morse, and C. A. Arrington, J. Chem. Phys. (submitted).
[47] J. M. Behm, M. A. Weibel, and M. D. Morse (unpublished).

Downloaded 02 Apr 2001 to 128.110.196.147. Redistribution subject to AIP copyright, see http://ojps.aip.org/jcpo/jcpcr.jsp